



e-ISSN: 2319-8753 | p-ISSN: 2347-6710

# IJRSET

International Journal of Innovative Research in  
**SCIENCE | ENGINEERING | TECHNOLOGY**

# INTERNATIONAL JOURNAL OF INNOVATIVE RESEARCH

IN SCIENCE | ENGINEERING | TECHNOLOGY

Volume 11, Issue 11, November 2022

**ISSN** INTERNATIONAL  
STANDARD  
SERIAL  
NUMBER  
INDIA

Impact Factor: 8.118

9940 572 462

6381 907 438

[ijrset@gmail.com](mailto:ijrset@gmail.com)

[www.ijrset.com](http://www.ijrset.com)



# Effect of RE Lanthanides Doping on Magnetic Properties of $MgFe_2O_4$ Nano-Ferrite

Umesh Chejara<sup>1</sup> • Anamika Prajapati<sup>2</sup> • Rupesh Kumar Basniwal<sup>3</sup>

<sup>1</sup>Department of Physics, University of Rajasthan, Jaipur 302004, India <sup>2</sup>Department of Chemistry, University of Rajasthan, Jaipur 302004, India, <sup>3</sup>AIARS (M&D), Amity University Uttar Pradesh, Noida, India

\*Corresponding author: [umeshchej@gmail.com](mailto:umeshchej@gmail.com) (Umesh Chejara)

## Abstract

Rare earth (RE) [Cerium ( $Ce^{3+}$ ) and Erbium ( $Er^{3+}$ )] lanthanides doped magnesium nanoferrites having the chemical composition  $MgCe_xEr_yFe_{2-x-y}O_4$  ( $x=0.4, 0.6, 0.8$  and  $y= 0.6, 0.4, 0.2$ ) have been synthesized by sol-gel method. These prepared nanoferrites series were studied by UV-Vis absorption, X-ray diffractometer (XRD), Fourier transform infrared spectroscopy (FTIR), Scanning electron microscopy (SEM) and magnetic properties of the prepared series were studied by the superconducting quantum interface device (SQUID) magnetometer. The M-H curve was plotted at different temperature (300 K, 100 K, 20 K and 5 K) measurements. The magnetic properties of prepared sample series saturation magnetization, retentivity and magnetic moment of the prepared nanoferrite studied in this literature. We finally envision that doping of rare earth (RE) ions ( $Ce^{3+}$  and  $Er^{3+}$ ) control the properties of magnesium ferrite samples and for future innovation.

**Keywords:** Sol-gel method, doping, rare earth elements, magnesium nano-ferrites and SQUID.

## 1. Introduction:

Metal oxide nanoparticles material is very useful in several applications in daily uses and research fields so needs to improve their properties. With the development of new technology its required high class of magnetic properties of material. Magnetic material is occupying an important place. The  $MgFe_2O_4$  normal magnesium spinal ferrite and it has cubic structure with properties of soft magnetic n-type semiconductor. This ferrite has wide range of applications like memory devices, microwave units, magnetic memory units, transformer, planer antennas, sensors and cancer treatment. [1] There are several methods of synthesis routes to producing magnesium ferrite spinel with desired properties like as hydrothermal technique in thin film and powder form, rapid solidification, high-temperature solid-state reaction, Electro-deposition, pulsed laser deposition, co-precipitation, sonochemical reactions, sol-gel method, combustion and high energy ball milling. Through wet chemical synthesis process we can enhance the material properties for example size, shape, phases and surface structure. This synthesis process provides fine tuning in reaction condition to achieve expected nanomaterials and these condition modify unconventional properties of material. In this paper, we are interested in developments of materials by the sol-gel auto combustion synthesis methods of nanoparticles to provide huge modification on the properties of prepared nanomaterials. In recent developments there are several methods to obtained metal oxide nanoparticles by wet chemical method but for scalable production to satisfy the growing industrial requirement of nanoparticles is sol-gel method and also special attention on low cost synthesis of nanoparticles. Ferrite are most important material which provide unique magnetic properties which is lies application in almost all fields and industry so no materials like ferrite wide range properties. [2] Spinel nanoferrites materials are very good class and stable material for research, technology and industrial uses like as biomedical, Radar



absorbing materials, microwave antenna information storage, pharmaceutical, MRI, high frequency power devices and remote sensing devices.[3-4]

Materials EM (electromagnetic) properties can be enhance by replacing or adding the various cations of the spinel ferrite also here is important factor that cations distribution its plays an important role in expected properties of nanoferrites. Here RE cations are also sourece of improvement of electromagnetic properties of preparing material. [5] The addition of RE elements into Mg-ferrite proved to strengthening, effective in grain refinement and anti-corrosion. By purification mechanisms, we can remove a part of impurity element and it is provides a way to advantage design of prepared material. Mg based alloys most popular research topic in current applications, weight reducing materials in engineering field and microwave antennas with negative refractive index materials by doping  $Ce^{3+}$  and  $Er^{3+}$  addition. [6] Ferrite materials has been also a huge interest in diverse technological field due to its high resistivity and low eddy current losses properties and Spinel ferrites important class of material which has chemically and thermally stable materials it makes uses of wide range of applications.[7]

By the comparison of magnetic properties of materials, the ferrimagnetic materials are more preferable due to its low eddy current and electromagnetic losses properties. Magnetic materials are very important class with nanosized dimension in various unique and remarkable applications. FCC (Face centre cubic) structure of spinel ferrite has chemical formula  $XFe_2O_4$  here 'X' represent metal cations for example  $Mg^{2+}$ ,  $Cd^{2+}$ ,  $Zn^{2+}$ ,  $Co^{2+}$ ,  $Mn^{2+}$ ,  $Ni^{2+}$  etc. It has been exhibits physical, chemical, optical, magnetic and dielectric behaviors are varied by its composition, substitution and synthesis process of materials. [8]

It's always interesting area for researchers of ferrites hexagonal-type crystal structures with interesting properties [9] so here we are also interested its electromagnetic properties which may be useful for microwave antennas material with negative refractive index and low energy loss and less heat extracting with communication process. This synthesis and study of  $MgCe_xEr_yFe_{2-x-y}O_4$  nanometer-sized ferrite particles focus on applied research work with special emphasis on their size dependent behavior. Nanoparticles  $MgCe_xEr_yFe_{2-x-y}O_4$  material series was prepared by the auto combustion sol-gel method. The average particle size of  $MgFe_2O_4$  nanoparticles was controlled through sol-gel process. The band gap of prepared series was determine by UV-Vis data with the help of Tauc plots and the FTIR measurements were conducted using Shimadzu spectrometer with a single reflection horizontal ATR accessory. The average particle size of prepared sample series were obtained by X-ray diffraction graph by the help of Scherrer relation and it is conformed to the help of SEM and magnetic properties were calculated from SQUID. The above studies will be helping us for design and construction for practical planer antenna application.

## 2. Experimental details:

### 2.1 Materials

The RE doped ferrites  $MgCe_xEr_yFe_{2-x-y}O_4$  achieved by Sol-Gel method and starting martial to synthesise purchased high purity metal nitrates from Sigma Aldrich Company (catalogue Nos.)

### 2.2 Synthesis of ferrite nanoparticles

The doped magnesium nanoparticles were synthesized following the methodology reported in the literature. Nanocrystalline powders of Ce and Er substituted magnesium nanoferrites with compositional formula  $MgCe_xEr_yFe_{2-x-y}O_4$  ( $x=0.4, 0.6, 0.8$  and  $y= 0.6, 0.4, 0.2$ ) were prepared by using sol-gel method. Mg nitrate hexahydrate and Fe nitrate hexahydrate were used as the precursors and RE,  $[Ce(NO_3)_2 \cdot 6H_2O]$  and  $[Er(NO_3)_3 \cdot 5H_2O]$  takes as dopants. Stoichiometric Amount of precursors metal nitrates were adds in pure water to achieve to clean solution. The Citric Acid mixed in water was added to the metal nitrate solution to disperse the NPs [10]. To obtain uniform solution of all aqueous solution of nitrates stirred on magnetic stirrer and gradually heated to  $80^\circ C$ . In order to make the solution



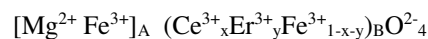
neutral (maintain the pH of solution 7) by adding required Ammonia (NH<sub>3</sub>) [11]. This solution was evaporated water molecules by raising temperature around 100°C on a heated plate with simultaneous stirring solution whenever solution does not changes into a viscous gel form and after some time all water molecules are vaporized from the solution by heating gel about 140°C. Then solution convert into viscous gel and this gel starts to indicate flameless combustion process take place with the releasing of huge amount of gases by change into dark brown coarse produce with looks like as a branched tree shape. Finally the burnt volumetric material powder was grounded and it was calcinate in atmosphere at 220°C for 4 hrs to achieve a spinel phase [12].

## 2.3 Characterization Technique

### 2.3.1 XRD analysis

The prepared Cerium and Erbium doped magnesium ferrite MgCe<sub>x</sub>Er<sub>y</sub>Fe<sub>2-x-y</sub>O<sub>4</sub> sample series via sol-gel route with concentration  $x$  and  $y$  ( $x=0.8, 0.6$  and  $0.4$  respectively  $y = 0.2, 0.4$  and  $0.6$ ). XRD (X-ray powder diffraction) data recorded and plotted by rigaku miniflex-600 diffraction spectrometer. This recorded spectrum helps us to determine diffraction planes, crystalline size and volume of cell of the prepared sample. The obtained XRD patterns of nanopowders were characterized by the use of Cu K- radiation of wavelength=1.5406 Å. The recorded XRD patterns presented by Figure 4 (a), (b) and (c) recorded peak exhibits around the (i) At diffraction angle  $2\theta = 29.36^\circ$  for the series  $X=0.8 Y=0.2$  (ii) At diffraction angle  $2\theta = 30.14^\circ$  for the series  $X=0.6 Y=0.4$  (iii) At diffraction angle  $2\theta = 30.48^\circ$  for the series  $X=0.4 Y=0.6$ , by the plane of (311), (220), (400), (422) and it is conformation that spinel structure of ferrite. [13] The analysis of XRD spectra provides their FCC structure and respective planes of nanoferrites. Peak pattern of XRD pattern exhibits the single phase and polycrystalline nature of prepared sample. to know magnetic properties of material it is necessary to know cations behave in spinel ferrite.

The spinel unit cell structure has included eight formula units and each unit cell has 64 A-sites (tetrahedral sites) and 32 B-sites (octahedral sites). The 1/2 parts of structure are fulfilling by octahedral sites and 1/8<sup>th</sup> part of structure are fulfilling by tetrahedral site from the cations



In above relation Ce<sup>3+</sup> and Er<sup>3+</sup> ions having inverse spinel structure and half part Fe<sup>3+</sup> ions fulfill tetrahedral site (A-site) and half part fulfill octahedral site (B-site). The nonmagnetic Mg<sup>2+</sup> ion have tendency occupy tetrahedral site. It is well known that more energy require for lanthanide substitution so that it will more thermal stable in comparison of unsubstantial ferrite material. Without doping material having large lattice constant and doped (Ce<sup>3+</sup> and Er<sup>3+</sup>) Mg –ferrite less lattice constant it represent they occupy octahedral site the same result reported in previous research work. [14]

Calculate the average their particle size by FWHM from X-ray pattern highest peak for (311) plane by using crystallite size software. This size is calculated on the basis of Scherrer's formula which is mentioned below equation [15,16]. Here (311) dominate peak due to Er<sup>3+</sup> doping and some more reflection peak appear in diffraction pattern due to oxides of doubly doped Ce<sup>3+</sup> and Er<sup>3+</sup> ions. The resultant value of average particle size are in range of 1.31nm ( $X=0.4 Y=0.6$ ) to 2.75nm ( $X=0.8 Y=0.2$ ) sample series and it is conform that the synthesized powder of Cerium and Erbium doped magnesium ferrite MgCe<sub>x</sub>Er<sub>y</sub>Fe<sub>2-x-y</sub>O<sub>4</sub> is of nanocrystalline particles and the average particle size increases with Ce<sup>3+</sup> concentration increases due to the larger ionic radius of Ce<sup>3+</sup> (1.15 Å) and Er<sup>3+</sup> (1.03 Å).

$$D = \frac{0.94\lambda}{\beta \cos\theta}$$



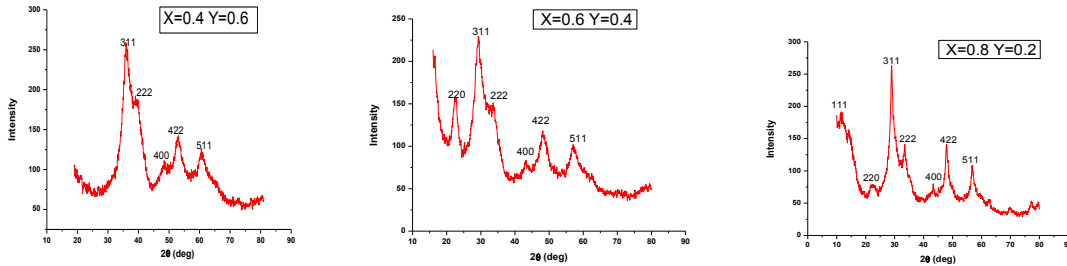


**Fig 1.** The XRD pattern of  $MgCe_x Er_y Fe_{2-x-y} O_4$  nano-ferrites powders for (a)  $X=0.4$   $Y=0.6$ , (b)  $X=0.6$   $Y=0.4$  and (c)  $X=0.8$   $Y=0.2$ .

By the above XRD figure 1 (a), (b) and (c) pattern shows that narrow reflection that is point out the narrow average crystallites size and average particle size increase as doping amount of  $Ce^{3+}$ . The average particle size of prepared sample between the scale of 1.31nm ( $X=0.4$   $Y=0.6$ ) to 2.75nm ( $X=0.8$   $Y=0.2$ ). The lattice parameter of prepares sample series increased with increasing of the  $Ce^{3+}$  ion doping amount. [17]

**Table no. 01 : XRD characterization comparison structure parameters for prepared series.**

S. No.	X value	Y value	particle size (nm)	lattice parameter (Å)	Volume(Å) <sup>3</sup>
1	0.8	0.2	2.75	10.09	1027.24
2	0.6	0.4	2.23	9.82	946.97
3	0.4	0.6	1.31	9.70	912.67

Source: These data taken from Rigaku miniflex-600 diffraction Spectrometer

### 2.3.2 Morphological analysis

The Cerium and Erbium doped magnesium ferrite  $MgCe_x Er_y Fe_{2-x-y} O_4$  nano powder studied by Scanning Electron Microscope (SEM- Zeiss evo 18) micrographs these images shown in Figure 1 (a), (b) and (c). These micrograph exhibits that there is presence of particles agglomerated together. [18] By the close study of micrograph reveal that there are presences of particles exhibits cubic faces and particles distribution is uniform. When the concentration is increase  $Er^{3+}$  or decrease concentration  $Ce^{3+}$  the average particle size are decrease as we know the atom size is larger for  $Ce^{3+}$  compare to the  $Er^{3+}$ . It is seen that the average particle size is below 40 nm, and it is similar result of grain size calculated in XRD by the Scherrer's relation. [19]

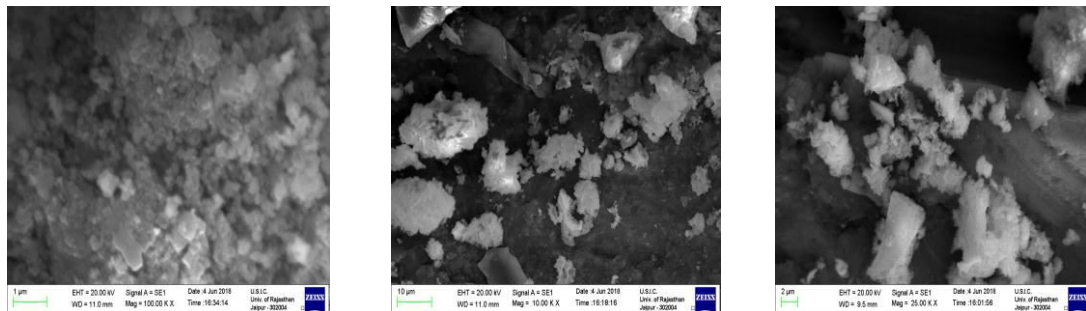


Fig 2. The SEM images of  $MgCe_x Er_y Fe_{2-x-y} O_4$  nano-ferrites powders for (a)  $X=0.4 Y=0.6$ , (b)  $X=0.6 Y=0.4$  and (c)  $X=0.8 Y=0.2$ .

### 2.3.3 UV Visible absorption analysis

The UV-Vis absorption spectrum as a function of wavelength for sample  $MgCe_x Er_y Fe_{2-x-y} O_4$  is shown in figure 3 (a),(b) and (c) having different value of x and y. For all the samples, highest absorption exhibits for the samples is at 222 nm wavelength.

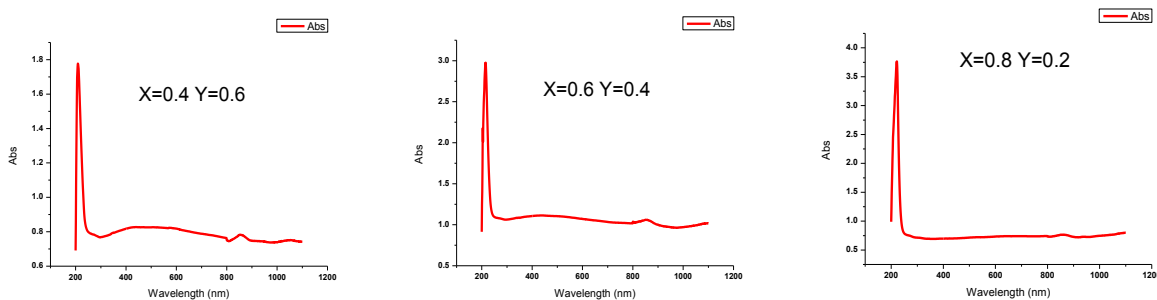
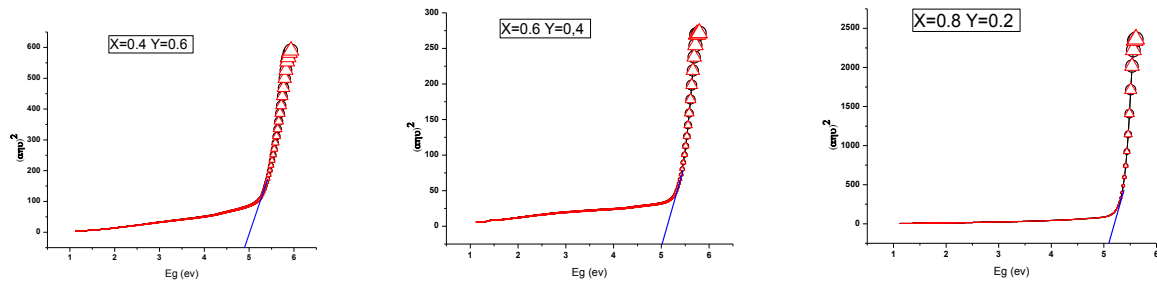


Fig 3. UV-Vis absorption spectra of doped magnesium nanoferrites sample,  $MgCe_x Er_y Fe_{2-x-y} O_4$  for (a)  $X=0.4 Y=0.6$ , (b)  $X=0.6 Y=0.4$  and (c)  $X=0.8 Y=0.2$ .

Several methods can be applied to examine the optical properties of prepared sample. But in all of methods mostly used method is the Tauc model its allow us to calculate  $E_g$  (band gap) energy by the term  $(ahv)^2$  by using data of incident energy ( $hv$ ). This Tauc band gap related with the  $MgCe_x Er_y Fe_{2-x-y} O_4$  sample ferrite is calculated by an extrapolation of the linear trend tracing in the Figure 4 of  $(ahv)^2$  curve in a selective interval of incident energies. This Tauc band gap is can be calculated by plotting the intercept of the linear extrapolation with Y axis. the term of  $(ahv)^2$  near the band edge absorption constant  $\alpha$  in several nano-ferrites exhibits exponential relation with incident energy obey the below relation :

$$(ahv) = A (hv - E_g)^n$$

Here A represent edge width parameter and absorption constant is  $\alpha$  and values of  $n = (1/2, 1, 2)$  is constant and taken values according to degree of transition.



**Fig 4.** Tauc plot of doped magnesium nanoferrites sample,  $MgCe_xEr_yFe_{2-x-y}O_4$  for (a)  $X=0.4$   $Y=0.6$ , (b)  $X=0.6$   $Y=0.4$  and (c)  $X=0.8$   $Y=0.2$ .

In this research work energy band gap calculated by Figures 4 (a), (b) and (c) plotted as incident energy versus  $(\alpha hv)^2$  by an extrapolating tangent line about the X-axis in Tauc plot [20] reveal in the Tauc plots for different stoichiometries of doped magnesium nanoferrites sample and we are found the energy band gaps 4.9, 5.0 and 5.1 eV respectively for prepared series with this concentrations ( $x = 0.4, 0.6$  and  $0.8$ ) [21].

### 2.3.4 Magnetic Measurements

The M-T curve (magnetization versus temperature) was plotted at different applied magnetic fields 50 Oe 500 Oe and 1000 Oe in the Figure 5 (a), (b) and (c). At Room temperature (300 K) M-H (magnetization versus magnetic field) curve were plotted for prepared Cerium and Erbium doped magnesium ferrite  $MgCe_xEr_yFe_{2-x-y}O_4$  nano powder and then plots M-H curve also for different temperature at 300 K, 100 K 20 K and 5 K. [22] by the plotted curve it seems to be typical S like hysteresis loops and very small values (near about zero) for coercivity and remanence values but there are magnetization very high at high applied field. [23] For prepared  $MgCe_xEr_yFe_{2-x-y}O_4$  nanoparticles plotted M-H graph show that for applied 50 Oe magnetic field nanomaterial shows blocking temperature decrease with decrease concentration of  $Ce^{3+}$  and others curves shows that increase applied magnetic field blocking temperature decrease that exhibits superparamagnetism at room temperature (300K) and also remains in same state down to 150K temperature. [24]. The  $M_s$  (saturation magnetization) value can be estimate by the hysteresis loop study of our sample exhibits that if a temperature increase the value of  $M_s$  Decrease for same concentration of series and it is also exhibits by plotted graph that  $M_s$  Value also decrease by decrease  $Ce^{3+}$  doping concentration. The value of  $M_s$  estimated by M versus applied magnetic field graph to  $1/H \rightarrow 0$  and the estimated values are listed in the Table 2.

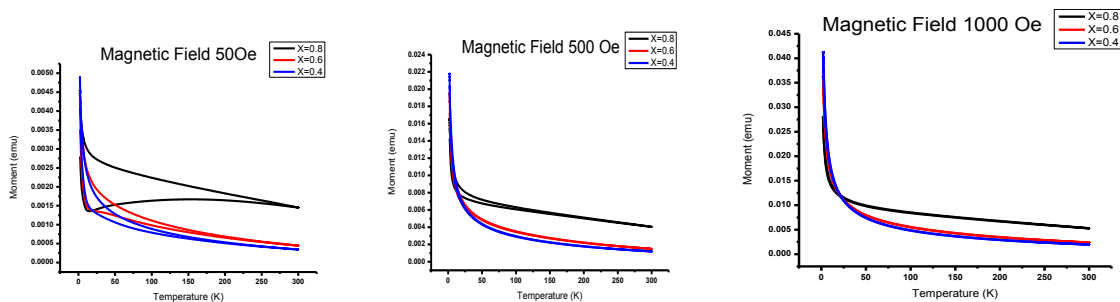


**Fig 5.** The zero-field-cooled (ZFC) curves measured from  $T = 10$  K to  $T = 300$  K in  $MgCe_xEr_yFe_{2-x-y}O_4$  nanoparticles at different applied magnetic fields of (a) 50Oe, (b) 500Oe and (c) 1000Oe.



Table no. 02 : variation of magnetic moment with varying applied magnetic field.

S.No.	Magnetic field	Maximum value of magnetic moment
1	50 Oe	0.0047 emu
2	500 Oe	0.022 emu
3	1000 Oe	0.042 emu

Source: These data collected by MPMS-3 SQUID Magnetometer

It is clear from table 3 that the highest estimated value of magnetic moment is 0.05 emu at 5K temperature and for the prepared series X=0.4 Y=0.6 and by the combine study of study prepared series increasing with temperature of sample the values of  $M_s$  decrease and variation in  $M_s$  also reported with variation applied magnetic field the highest values reported in table 3 at 1000 Oe is 0.042 emu. If change the applied magnetic field for prepared sample Cerium and Erbium doped magnesium ferrite  $MgCe_xEr_yFe_{2-x-y}O_4$  the time dependent effect exhibits and magnetic moment reorient and domain walls moves with two type of resonance. First one is spin and second is domain wall resonance. The spin rotate slowly is order of  $10^7-10^8 s^{-1}$ . It is representing that relaxation frequency does not provide critical damping. In ferrite a magnetic inert component introduce then it is magnetic dilution and also a cut off the magnetic circuit for the ferrite, so ferrite volume loading decreases result permeability is reduced. We can say the other reason is low volume composite materials have individual magnetic particle separation due to this magnetic pole of every particle generated the demagnetization field. Therefore a change in applied magnetic field its result is ferrite respond to magnetization relaxation as globus model [17].

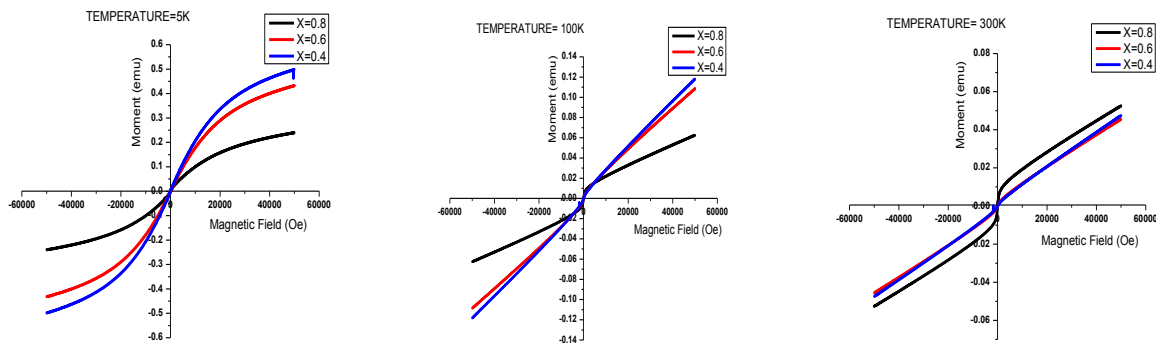


Fig 6. Hysteresis curve comparison for series at constant temperature (a) T=5K, (b) T=100K and (c) T=300K.

Table no. 03 : Magnetic moment values with increasing temperature in emu/gm units.

S.No.	Temperature(K)	X=0.4 Y=0.6 magnetic moment ( $\mu_B$ )	X=0.6 Y=0.4 magnetic moment ( $\mu_B$ )	X=0.8 Y=0.2 magnetic moment ( $\mu_B$ )
1	5 K	100 emu/gm	84 emu/gm	40 emu/gm
2	20 K	70 emu/gm	60 emu/gm	30 emu/gm
3	100 K	24 emu/gm	22 emu/gm	12 emu/gm
4	300 K	8 emu/gm	7.6 emu/gm	10 emu/gm

Source: These data collected by MPMS-3 SQUID Magnetometer





The saturation magnetization ( $M_s$ ) of Mg–Fe ferrite materials was calculated by the prepared hysteresis loop. The magnetic moment ( $n_B$ ) values in ( $\mu_B$ ) calculated by using below relation [25]

$$n_B = \frac{M_w t \times M_s}{5585}$$

Here,  $M_w$  represent molecular weight. Magnetic moments for variation with temperature listed in Table 5.

**Table no. 04 : Magnetic moment values with increasing temperature in  $\mu_B$  units.**

S.No.	Temperature(K)	X=0.4 Y=0.6 magnetic moment ( $n_B$ )	X=0.6 Y=0.4 magnetic moment ( $n_B$ )	X=0.8 Y=0.2 magnetic moment ( $n_B$ )
1	5 K	5.38	4.52	2.15
2	20 K	3.76	3.23	1.61
3	100 K	1.29	1.18	0.64
4	300 K	0.43	0.41	0.54

Source: These data collected by MPMS-3 SQUID Magnetometer

Highest value of saturation magnetization value is 100 emu/gm for sample X=0.4 Y=0.6 at 5K temperature corresponding magnetization value 55000 G the value of magnetic susceptibility ( $\chi$ ) calculate by this formula

$$\chi = \frac{B}{H}$$

The value of  $\chi$  is 0.00023057 and corresponding magnetic permeability ( $\mu$ ) obtain 1.002898 it has been exhibits that increase the doping and temperature too  $\mu$  increase. [17]

The different parameters such as maximum magnetic moment are presented in Table 3 and 4 in different units. By the present study it is seems to be magnetic properties altered by  $Ce^{3+}$  and  $Er^{3+}$  doped Magnisium ferrite and By the study of magnetic properties the saturation magnetization values increased by the adding of  $Ce^{3+}$  and  $Er^{3+}$  doping this result reported in Rezlescu et al. [26] Lanthanides  $Ce^{3+}$  and  $Er^{3+}$  doped Mg ferrite have higher values of saturation magnetization in comparison of without doping ferrite this similar results presented by Liu et al. [27] and if increases temperature paramagnetic behavior exhibits and increasing  $Ce^{3+}$  concentration also behave turn into ferromagnetic to paramagnetic properties. These above graphs are plotted at constant temperature 5K 20K 100K and 300K these curves shows that the slope of curve decreases as increase temperature and represent lower values for prepared series X=0.8,Y=0.2 that mean ferromagnetic properties of material is converting into paramagnetic properties and growth of domain is also decreases.

### Conclusions:

The  $MgCe_xEr_yFe_{2-x-y}O_4$  lanthanide doped nanoparticles was prepared successfully by using sol-gel root by the concentration of series X=0.4, 0.6, 0.8 and Y=0.6, 0.4, 0.2 respectively. The structural properties of spinel ferrites depend on mainly method of preparation. The prepared single phase crystallite structure nanomaterial series have average size obtained 1.31 - 2.75 nm was confirmed by X-ray diffraction results and also provides supported result for SEM. It is exhibit that the lattice parameter decrease with decreasing concentration of  $Ce^{3+}$  and  $Er^{3+}$  ions it is due to large ionic radius of  $Ce^{3+}$  (1.15 Å) and  $Er^{3+}$  (1.03 Å) in compare of host cation i.e.,  $Mg^{2+}$  (0.86 Å) and  $Fe^{3+}$  (0.69 Å). There is also decrees lattice parameter for prepared  $Ce^{3+}$  and  $Er^{3+}$  doped magnesium ferrite with increase  $Er^{3+}$  or decrease  $Ce^{3+}$  ions numbers and the reason of this grater radius of  $Ce^{3+}$  ions as compare to  $Er^{3+}$  ions. By UV-Vis study optical band gap energy lies between 4.9 to 5.1 eV for prepared series for different lanthanide doping concentration. Magnetic permeability ( $\mu$ ) values obtain 1.002898 and it is slightly varies with doping concentration. The desired synthesized nanoferrites results are very useful many areas in planer antenna and technological instrumentions like soft magnets, microwave devices, remote sensing and magnetic fluids for hyperthermia.



### Acknowledgments

U.C. acknowledges University of Rajasthan for providing all the necessary research facilities and also acknowledges Dr. K V R Rao and Dr. V K Saxena from University of Rajasthan for their valuable guidance and helpful discussions.

### References:

1. J. Govha ,T. Bala Narasaiah, P. Kumar , C. Shilpa Chakra, Synthesis of Nano-Magnesium Ferrite Spinel and its Characterization International, Journal of Engineering Research & Technology (IJERT) **3**, 1420 (2014)
2. R. Vemuria, G. Rajub, M. Gnana Kiranc, M.S.N.A. Prasadd, E. Rajeshb, G. Pavan Kumare, N. Muralif, Effect on structural and magnetic properties of Mg<sup>2+</sup> substituted cobalt nano ferrite, Elsevier Results in Physics **12**, 947-952 2018 <https://doi.org/10.1016/j.rinp.2018.12.032>.
3. Q. A. Pankhrust, J. Connolly, S. K. Jones, J. Doobson, Applications of magnetic nanoparticles in biomedicine, J. Phys. D: Appl. Phys. **36**, 167 (2003)
4. Q. Chen, Z. J. Zhang, Size-dependent super paramagnetic properties of spinel ferrite nanocrystallites, Appl. Phys. Lett. **73**, 3156 (1998)
5. M. Junaid, M. A. Khan, F. Iqbal, G. Murtaza, M. N. Akhtar, M. Ahmad, I. Shakir, M. F. Warsi, Structural, spectral, dielectric and magnetic properties of Tb–Dy doped Li–Ni nano-ferrites synthesized via micro-emulsion route, J. Magn. Magn.Mater. **419** 338-344 (2016)
6. J. Zheng, B. Chen, Unexpected Fe-Enriched Compounds Observed in Mg–Ce Alloy: An Atomic-Scale STEM Investigation, Wiley Periodicals, Inc. **9999** 783–791 (2016) <https://doi.org/10.1002/sca.21328>
7. R. Srivastava, B. C. Yadav, Ferrite Materials: Introduction, Synthesis Techniques, and Applications as Sensors, International Journal of Green Nanotechnology, **4** 141-154 (2012) <http://dx.doi.org/10.1080/19430892.2012.676918>.
8. M. N. Akhtara, M. A. Khan, Effect of rare earth doping on the structural and magnetic features of nanocrystalline spinel ferrites prepared via sol gel route, Journal of Magnetism and Magnetic Materials (2018) <https://doi.org/10.1016/j.jmmm.2018.03.069>
9. M. Mahdiani, A.Sobhani, Masoud, The first synthesis of CdFe<sub>12</sub>O<sub>19</sub> nanostructures and nanocomposites and considering of magnetic, optical, electrochemical and photocatalytic properties, Journal of Hazardous Materials (2019) <https://doi.org/10.1016/j.jhazmat.2019.01.007>
10. M. K. Shobana, K. Kim, J. H. Kim, Impact of Magnesium substitution in Nickel ferrite, Optical and Electrochemical Studies, Physica E: Low-dimensional Systems and Nanostructures (2018) <https://doi.org/10.1016/j.physe.2018.12.013>
11. M. I. M. Omer, A. A. Elbadawi, O. A. Yassin, Synthesis and Structural Properties of MgFe<sub>2</sub>O<sub>4</sub> Ferrite Nano-particles, Journal of Applied and Industrial Sciences **1(4)** 20-23 (2013)
12. M. Raghasudha, D. Ravinder, P. Veerasomaiah<sup>1</sup>, S. goud, G. S. Goud, B. Rambabu<sup>1</sup>, N. Venkatesh, Synthesis and Magnetic properties of CoFe<sub>2</sub>O<sub>4</sub> and MgFe<sub>2</sub>O<sub>4</sub> spinel nano ferrites, ResearchGate NCRAANM (2016) <https://www.researchgate.net/publication/308948082>
13. K. Muthuraman, V. Naidu, S. K. A. Ahamed, K. Sahib, Study of Electrical and Magnetic Properties of Cerium Doped Nano Smart Magnesium Ferrite Material, International Journal of Computer Applications **65** 18-24 (2013)
14. M. Gateshki, V. Petkov, S. K. Pradhan, T. Vogt, Structure of nanocrystallineMgFe<sub>2</sub>O<sub>4</sub> from X-ray diffraction, Rietveld and atomic pair distribution function analysis, Journal of Applied Crystallography **38** 772-779 (2005) <https://doi.org/10.1107/S0021889805024477>
15. C. B. D., Elements of X-Ray Diffraction, Addison Wesley Pub. Co. Inc., London (1967), pp 259-269



16. C.O. Ehi-Eromosele<sup>1</sup>, J.A.O. Olugbuyiro<sup>1</sup>, O.S. Taiwo, O.A. Bamgboye and C.E. Ango, Synthesis And Evaluation Of The Antimicrobial Potentials Of Cobalt Doped- And Magnesium Ferrite Spinel Nanoparticles, Chemical Society of Ethiopia and The Authors **32(3)**, 451-458 (2018) <https://dx.doi.org/10.4314/bcse.v32i3.4>
17. S.K.A. Ahamed Kandu Sahib , M. Sharon Eloise Violet, T.Sheeba S.Usha Rani, Preparation, Characterization and Electrical Properties Studies of Nano Sized Cerium Neodymium Doped Magnesium Ferrite SSRG International, Journal of Electronics and Communication Engineering **40**, 7-12 (2018)
18. S.G.C. Fonseca, L. S. Neiva, M.A.R. Bonifacio, P. R.C. Santosa, U.C. Silva, J. B. L. O. Tunable Magnetic and Electrical Properties of Cobalt and Zinc Ferrites CO<sub>1</sub>-xZnXFe<sub>2</sub>O<sub>4</sub> Synthesized by Combustion Route, Materials Research, **21(3)** 1-9 (2018) <http://dx.doi.org/10.1590/1980-5373>
19. S.Y. Mulushoa, M. T. Wegayehu, G. Tewodros Aregai, N. Murali, M. Sushma Reddi, B. V. Babu, T. Arunamani and K. Samatha, Synthesis of Spinel MgFe<sub>2</sub>O<sub>4</sub> Ferrite Material and Studying its Structural and Morphological Properties Using Solid State Method, Chemical Science Transactions **6(3)**, 1-8 (2017) <https://doi.org/10.7598/cst2017.1401>
20. D. Yuliantika, A. Taufiq, A. Hidayat, Sunaryono, N. Hidayat, S. Soontaranon, Exploring Structural Properties of Cobalt Ferrite Nanoparticles from Natural Sand IOP Conf. Series: Materials Science and Engineering **515**,1-11 (2018) <https://doi.org/10.1088/1757-899X/515/1/012047>
21. A. I. Ahmed, M. A. Siddig, A. A. Mirghni, M. I. Omer, A. A. Elbadawi, Structural and Optical Properties of Mg<sub>1-x</sub>Zn<sub>x</sub>Fe<sub>2</sub>O<sub>4</sub> Nano-Ferrites Synthesized Using Co-Precipitation Method, Advances in Nanoparticles, **4**, 45-52 (2015) <http://dx.doi.org/10.4236/anp.2015.42006>
22. M. Buchner, K. Hofler, B. Henne, V. Ney, and A. Ney, Tutorial: Basic principles, limits of detection, and pitfalls of highly sensitive SQUID magnetometry for nanomagnetism and spintronics, Journal Of Applied Physics **124**, 16110101-1611012 (2018) <https://doi.org/10.1063/1.5045299>
23. M. Raghasudha, D. Ravinder, P. Veerasomaiah, S. Goud, G. S. Goud, B. Rambabu, N. Venkatesh, Synthesis and Magnetic properties of CoFe<sub>2</sub>O<sub>4</sub> and MgFe<sub>2</sub>O<sub>4</sub> spinel nano ferrites, Researchgate (2016) <https://www.researchgate.net/publication/308948082>
24. G. Lal, K. Punia, S. N.Dolia, P.A. Alvi, S. Dalela, S. Kumar, Rietveld refinement, Raman, optical, dielectric, Mössbauer and magnetic characterization of superparamagnetic fcc-CaFe<sub>2</sub>O<sub>4</sub> nanoparticles Elsevier **45**, 5837-5847 (2019) <https://doi.org/10.1016/j.ceramint.2018.12.050>
25. A. M. Mohammad , S. M. Ali Ridha, T. H. Mubarak, Structural And Magnetic Properties Of Mg-Co Ferrite Nanoparticles Digest Journal of Nanomaterials and Biostructures **13**, 615-623 (2018)
26. N. Rezlescu, E. Rezlescu, C. Pasnicu, M.L. Crau, Effect of the rare-earth ions on some properties of nickel-zinc ferrite, J. Phys. Condens. Matter **6**, 5707 (1994)
27. X. Liu, W. Zhong, S. Yang, Z. Yu, B. Gu, Y. Du, Influence of La<sup>3+</sup> substitution on the structural and magnetic properties of M-type strontium ferrites, J. Magn. Magn. Mater **238**, 207-214 (2002)



**INNO SPACE**  
SJIF Scientific Journal Impact Factor  
**Impact Factor: 8.118**



**ISSN** INTERNATIONAL  
STANDARD  
SERIAL  
NUMBER  
INDIA



# INTERNATIONAL JOURNAL OF INNOVATIVE RESEARCH

IN SCIENCE | ENGINEERING | TECHNOLOGY

 **9940 572 462**  **6381 907 438**  **ijirset@gmail.com**



[www.ijirset.com](http://www.ijirset.com)

Scan to save the contact details